Chemical Science

ROYAL SOCIETY OF CHEMISTRY

EDGE ARTICLE

View Article Online
View Journal | View Issue

Cite this: *Chem. Sci.*, 2024, **15**, 4846

All publication charges for this article have been paid for by the Royal Society of Chemistry

Mitochondria-targeting biocompatible fluorescent BODIPY probes†

Edward R. H. Walter, ‡[ab] Lawrence Cho-Cheung Lee, ‡[bc] Peter Kam-Keung Leung, [cd] Kenneth Kam-Wing Lo *[cd] and Nicholas J. Long *[a]

An increase in the mitochondrial membrane potential (MMP) is a characteristic feature of cancer and cardiovascular disease. Therefore, it remains of crucial importance to develop new and improved fluorescent probes that are sensitive to the MMP, to report on mitochondrial health and function. Reported here are the design, synthesis, photophysical properties and biological characterisation of a series of BODIPY dyes, **BODIPY-Mito-*n***, for mitochondria-targeted fluorescence imaging applications. Six **BODIPY-Mito-*n*** analogues were synthesised under mild conditions, and displayed excellent fluorescence quantum yields of between 0.59 and 0.72 in aqueous environments at physiological pH (pH = 7.4). The incorporation of poly(ethylene glycol) (PEG) chains to the triarylphosphonium cation moiety significantly improved the biocompatibility of the probes (**BODIPY-Mito-6**, IC_{50} > 50 μM). All **BODIPY-Mito-*n*** compounds demonstrated a high MMP-sensitive localisation in the mitochondria, with Pearson's correlation coefficients (PCC) of between 0.76 and 0.96. Compounds **BODIPY-Mito-2** and **BODIPY-Mito-6** revealed the highest sensitivity to the MMP, with a decrease in the emission intensity of 62% and 75%, respectively following MMP depolarisation. It is anticipated that the highest MMP sensitivity and enhanced biocompatibility of **BODIPY-Mito-6** could lead to the development of new probes for mitochondrial imaging in the future.

Received 1st December 2023
Accepted 17th February 2024

DOI: 10.1039/d3sc06445j

rsc.li/chemical-science

Introduction

Mitochondria are important subcellular organelles, most notable for their key role in ATP generation *via* oxidative phosphorylation.[1] Since this discovery in 1957, the role of mitochondria is known to be considerably more complex, with mitochondrial function and dysfunction now recognised to act as important factors in cancer cell metabolism,[2] neurodegeneration[3] and aging.[4]

Mitochondria have a negative mitochondrial membrane potential (MMP, $\Delta\Psi_m$), facilitating a stepwise accumulation of lipophilic cations into the mitochondrial matrix in accordance with the Nernst equation.[5] The conjugation of a lipophilic cation, such as triphenylphosphonium (TPP^+) to small molecules increases their accumulation in the mitochondrial matrix by 1000-fold compared to the extracellular space.[6]

Healthy cells have an MMP between −150 and −180 mV.[7] In both cancer and cardiovascular disease, the MMP is known to increase considerably,[8] enabling compounds that accrue in the mitochondria in an MMP-dependent manner to be utilised for non-invasive imaging of mitochondrial function, and the delivery of therapeutic cargo.[9] For example, such an approach has been utilised for a wide range of imaging agents to study mitochondrial dysfunction by Single-Photon Emission Computed Tomography[10] and Positron Emission Tomography (PET).[11–14]

Fluorescence Imaging (FI) is an important and powerful imaging technique with a high sensitivity and spatial resolution.[15] A wide range of cationic and lipophilic fluorescent probes have been developed for selective mitochondria imaging, and a number of which are commercially available. Mitochondria-targeting probes can be broadly divided into two main groups: firstly, compounds that demonstrate an MMP-dependent uptake and retention in the mitochondria, such as JC-1[16] and rhodamine 123.[17] Secondly, probes have been designed to bind covalently to mitochondrial proteins, as epitomised by the MitoTracker™ series,[18] but they cannot provide direct information on mitochondrial function.

Boron-dipyrromethenes (BODIPYs) are an important class of widely studied fluorescent dyes characterised by high extinction coefficients, excellent thermal- and photo-stability and high

[a]*Department of Chemistry, Imperial College London, Molecular Sciences Research Hub, London, W12 0BZ, UK. E-mail: n.long@imperial.ac.uk*

[b]*Laboratory for Synthetic Chemistry and Chemical Biology Limited, Units 1503-1511, 15/F, Building 17 W, Hong Kong Science Park, New Territories, Hong Kong, P. R. China*

[c]*Department of Chemistry, City University of Hong Kong, Tat Chee Avenue, Kowloon, Hong Kong, P. R. China*

[d]*State Key Laboratory of Terahertz and Millimetre Waves, City University of Hong Kong, Tat Chee Avenue, Kowloon, Hong Kong, P. R. China*

† Electronic supplementary information (ESI) available. See DOI: https://doi.org/10.1039/d3sc06445j

‡ Equal contribution from both authors.

fluorescence quantum yields (ϕ).[19,20] Additionally, the core structure can be easily modified to tune the photophysical properties[21,22] and introduce biological targeting moieties.[23] Over the last decade, a wide range of BODIPY-based mitochondria-targeting compounds were developed,[24–29] including probes for dual-modal PET/FI,[26,27] and to report on mitochondrial reactive oxygen species such as hypochlorous acid[28] and peroxynitrite.[29]

To date, one major problem in this area of research is the development of new and improved fluorescent probes with an MMP-dependent uptake. Historically, the accumulation and retention of BODIPY-based compounds is either independent of the MMP,[24,26] or the experiments to determine this sensitivity are not carried out,[25,27] limiting the use of these probes to report on mitochondrial function.

In 2016, Archibald and co-workers reported the first BODIPY-based probes demonstrating an MMP-dependent accumulation and retention in the mitochondria (**BODIPY-I** and **BODIPY-II**, Fig. 1A).[30] It was determined that **BODIPY-I**, containing two cyclohexyl moieties, displayed a greater than 70% decrease in mean fluorescence intensity in cancer (MCF-7) and heart (H9c2) cells following mitochondrial depolarisation. Additionally, a BODIPY analogue bearing a [^{19}F]-fluorobutyl moiety showed significant promise towards the synthesis of a dual-modal PET/FI probe.[30] However, the late stage installation of a dicyclohexylphosphine or diphenylphosphine moiety with *n*-butyllithium required the modification of the BODIPY core prior to lithiation.[31]

Previous studies have also demonstrated that B–F substitution with phenyl or methyl substituents significantly reduced the fluorescence quantum yields.[31,32] Additionally, such a modification hinders further structural adjustment, for example, the introduction of water solubilising groups onto the boron centre.[33,34]

Here we report the design, synthesis, photophysical properties and biological characterisation of a series of **BODIPY-Mito-*n*** compounds bearing cyclohexyl and/or phenyl moieties (Fig. 1B) to determine the optimum substitution requirements for high mitochondrial localisation and MMP sensitivity. We envisaged that commercially available cyclohexyl- and phenyl-substituted phosphines can be introduced to the BODIPY core *via* nucleophilic substitution under mild basic conditions, without the need for prior B–F substitution. The use of mild conditions also enabled the development of BODIPY analogues containing triarylphosphines incorporating di(ethylene glycol) (DEG) (**BODIPY-Mito-5**) and poly(ethylene glycol) (PEG) moieties (**BODIPY-Mito-6**) (Fig. 1B) to determine how the length of the chain modifies the mitochondrial uptake and retention of the probes following MMP reduction.

Finally, to confirm the importance of the phosphonium cation in facilitating mitochondrial localisation, **BODIPY-Et** (Fig. 1B) was synthesised for comparison studies.

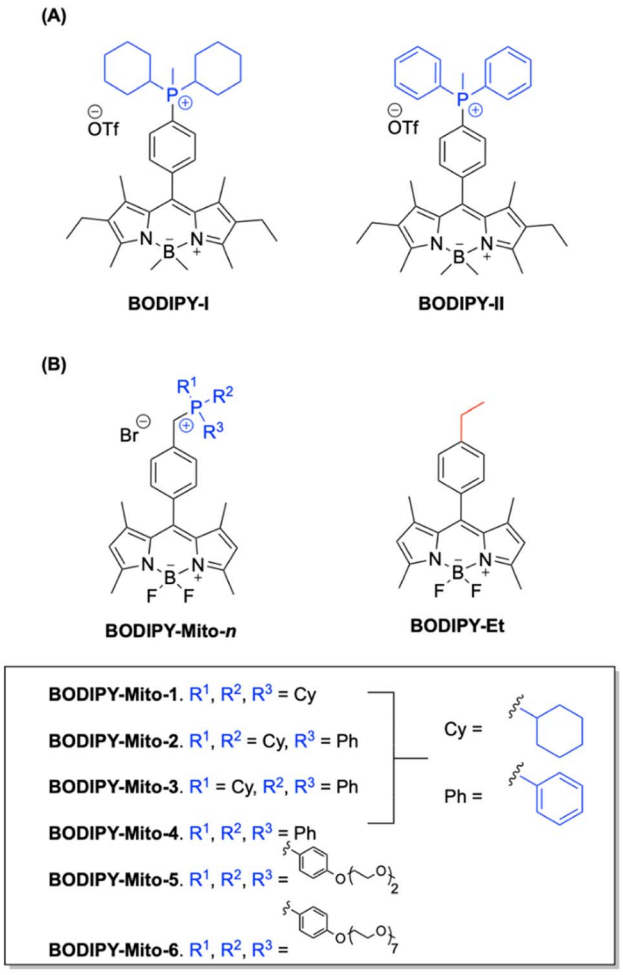

Fig. 1 Phosphonium cation-functionalised BODIPY compounds. (A) Previously reported compounds by Archibald and co-workers,[30] and (B) BODIPY-Mito-*n* compounds investigated in this work.

Results and discussion

Design and synthesis of BODIPY-Mito-*n* analogues

The synthesis of **BODIPY-Mito-*n*** is shown in Scheme 1. Briefly, in a procedure adapted from Zhang and co-workers,[35] **BODIPY-Br** was formed in a one-pot condensation reaction with 2,4-dimethylpyrrole and (**1**)[36] in reasonable yields following purification by silica-gel column chromatography.

Phosphines bearing cyclohexyl or phenyl functionalities were purchased from commercial suppliers, and DEG-based aryl phosphine, compound (**2**), was synthesised as first described by Wang and co-workers (ESI, Scheme S1†).[37] The synthesis of (**7**) was achieved using a similar procedure to that of (**2**), but instead using a PEG unit with an average molecular weight of 350 Da (PEG-350).

Subsequent nucleophilic substitution of **BODIPY-Br** with phosphine precursors ($PR^1R^2R^3$) formed **BODIPY-Mito-*n*** analogues in good yields (50–92%) (Scheme 1). Reactions with phosphines containing cyclohexyl moieties were undertaken in toluene, and purified by recrystallisation in dichloromethane and hexane. However, for the aryl phosphine analogues, **BODIPY-Mito-4**, **BODIPY-Mito-5** and **BODIPY-Mito-6**, it was found that higher yields were achieved when the reactions were performed in acetonitrile.

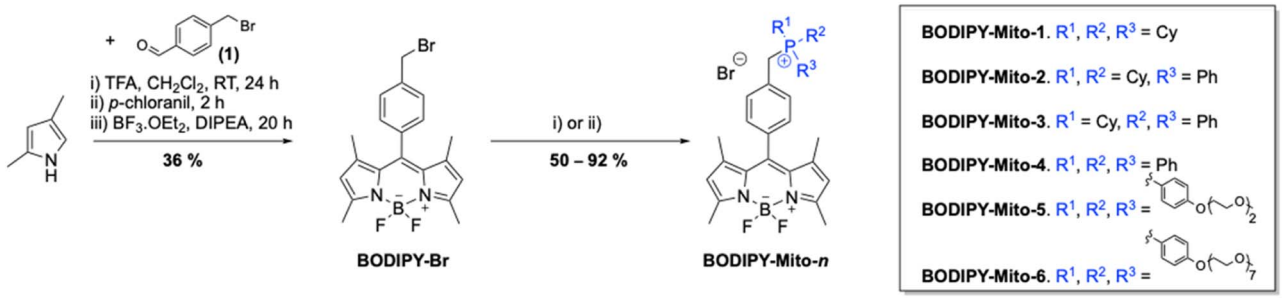

Scheme 1 Synthesis of **BODIPY-Mito-*n***. Conditions: (i) $PR^1R^2R^3$, toluene, 110 °C, 3 d (**BODIPY-Mito-1–3**) and (ii) $PR^1R^2R^3$, CH_3CN, 85 °C, 3 d (**BODIPY-Mito-4–6**).

Finally, **BODIPY-Et** was synthesised in an analogous manner to **BODIPY-Br**, but instead using 4-ethylbenzaldehyde (Scheme S2†). However, rather than a one-pot reaction, higher yields were achieved following purification of the dipyrromethane intermediate *via* silica-gel column chromatography prior to complexation with boron trifluoride etherate under basic conditions.

Photophysical properties of BODIPY-Mito-*n* analogues

The photophysical properties of the BODIPY compounds synthesised in this study were recorded in PBS (pH = 7.4) to simulate physiological conditions, and acetonitrile (detailed in the ESI†) for comparison.

The absorption, emission and excitation spectra of **BODIPY-Mito-1** in PBS are shown in Fig. 2, displaying a characteristic absorption maximum at 497 nm and a fluorescence maximum at 511 nm. As expected, all **BODIPY-Mito-*n*** analogues demonstrated almost identical absorbance, emission and excitation wavelength maxima in PBS (pH = 7.4) (Table 1 and Fig. S1†) and acetonitrile (Table S1 and Fig. S2†).

Additionally, all analogues were found to have extinction coefficients in the range of 5.56–6.49 × 10^4 M^{-1} cm^{-1}, and high fluorescence quantum yields between 0.59 and 0.72 in aqueous media (Table 1). Interestingly, the highest quantum yield of 0.72 was reported for the PEGylated (PEG-350) analogue **BODIPY-Mito-6**. Finally, the absorption and emission spectra of **BODIPY-Mito-*n*** analogues were found to be independent of pH in the physiological range (pH 5–8) (Fig. S4–S6†).

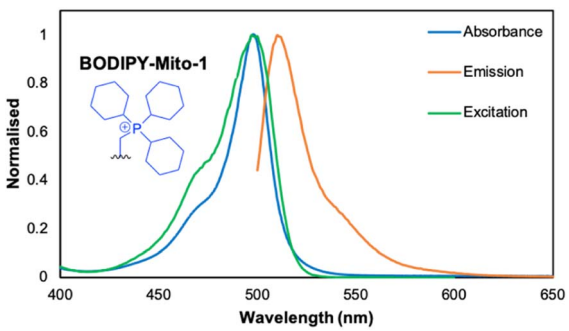

Fig. 2 Absorption (blue), emission (orange) and excitation (green) spectra of **BODIPY-Mito-1**. [BODIPY] = 10 μM, PBS (pH = 7.4), 298 K. λ_{ex} = 497 nm, λ_{em} = 511 nm.

Table 1 Photophysical data for **BODIPY-Mito-*n*** compounds and **BODIPY-Et** discussed in this study[a]

BODIPY	λ_{abs}/nm (ε/10^4 M^{-1} cm^{-1})	λ_{ex}/nm	λ_{em}/nm	QY (ϕ)
BODIPY-Mito-1	497 (5.56)	497	511	0.60
BODIPY-Mito-2	497 (6.45)	497	511	0.67
BODIPY-Mito-3	497 (6.40)	497	511	0.62
BODIPY-Mito-4	497 (5.92)	497	511	0.59
BODIPY-Mito-5	497 (5.67)	497	512	0.62
BODIPY-Mito-6	498 (6.49)	500	512	0.72
BODIPY-Et	488 (3.83), 538 (5.74)[b]	—[c]	—[d]	—[c]

[a] [BODIPY] = 10 μM in PBS (pH = 7.4), 298 K, λ_{ex} = 497 nm. Quantum yields (QY) (ϕ) were measured using fluorescein in 0.1 M NaOH ($\phi_{496\ nm}$ = 0.95)[38] as the standard. Estimated error = ±20%. [b] Broad absorption spectrum. [c] Not measured. [d] Very weak emission was observed.

BODIPY-Et, in comparison, displayed markedly different photophysical properties in PBS (pH 7.4). The absorption band became significantly broader with the absorption maximum located at 538 nm. Furthermore, **BODIPY-Et** was notably less soluble in aqueous environments and very weakly fluorescent. However, in acetonitrile similar absorption, emission and excitation wavelength maxima were displayed (Table S1 and Fig. S3†). Such a discrepancy in aqueous media is likely due to an increase in π–π aggregation caused by the higher lipophilicity of **BODIPY-Et**.

Imaging of BODIPY-Mito-*n* analogues in living cells

The cellular uptake and localisation properties of the **BODIPY-Mito-*n*** compounds were studied by laser-scanning confocal microscopy (LSCM) and flow cytometry using HeLa cells as a model. Upon incubation of HeLa cells with **BODIPY-Mito-1–4** (500 nM, 1 h), intense emission was observed in the perinuclear region of the cells with negligible nuclear uptake (Fig. 3A). As indicated by flow cytometry, the treated cells displayed similar intracellular emission intensities (Fig. 3B), suggestive of a similar rate of cellular uptake among these compounds. To confirm the specific localisation of **BODIPY-Mito-1–4**, the cells were co-stained with the commercially available mitochondrial stain MitoTracker Deep Red.

Strikingly, **BODIPY-Mito-1–4** were specifically accumulated in the mitochondria of the cells with Pearson's correlation coefficients (PCCs) ranging from 0.92 to 0.96 (Fig. 4). These

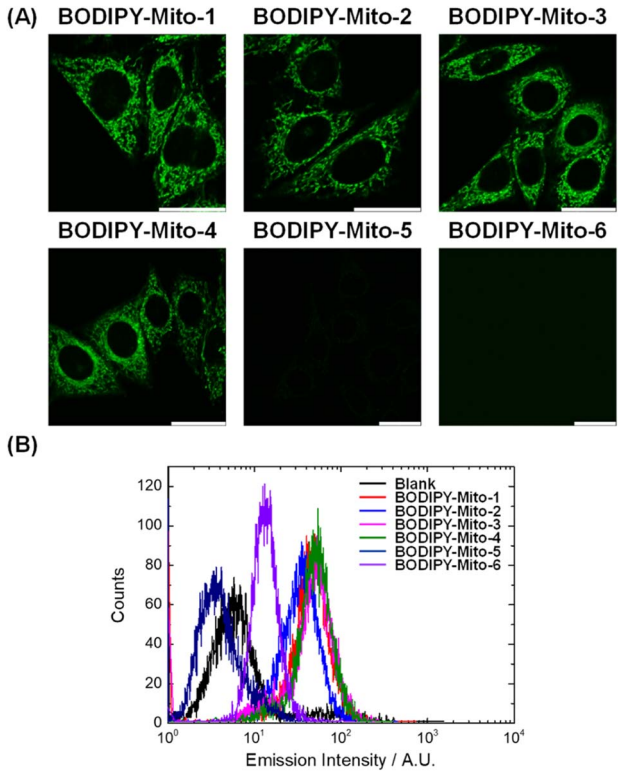

Fig. 3 (A) LSCM images of live HeLa cells incubated with **BODIPY-Mito-*n*** (500 nM, 1 h) at 37 °C. λ_{ex} = 488 nm, λ_{em} = 501–521 nm. Scale bar = 25 μm. (B) Flow cytometric results of HeLa cells incubated with blank medium or **BODIPY-Mito-*n*** (500 nM, 1 h) at 37 °C.

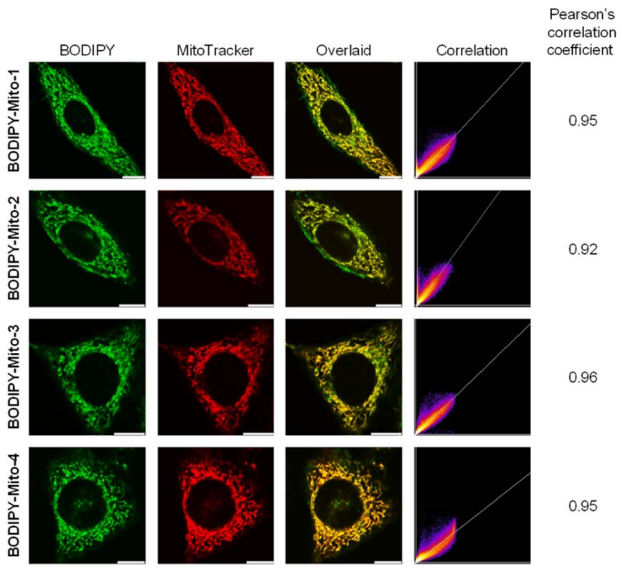

Fig. 4 LSCM images of live HeLa cells incubated with **BODIPY-Mito-1–4** (500 nM, 1 h; λ_{ex} = 488 nm, λ_{em} = 501–521 nm) and then MitoTracker Deep Red (100 nM, 30 min; λ_{ex} = 635 nm, λ_{em} = 655–675 nm) at 37 °C. Scale bar = 10 μm.

results confirm that both cyclohexyl and phenyl moieties on the phosphonium cation can realise high accumulation of the probes in the mitochondria. Such a result further supports observations by Rokitskaya and co-workers, that the aromaticity of lipophilic cations is not important for effective permeation through lipid membranes and accumulation in the mitochondria.[39]

However, treatment of HeLa cells with **BODIPY-Mito-5** and **BODIPY-Mito-6**, which contain three DEG and PEG chains, respectively, gave negligible intracellular emission under the same conditions (Fig. 3A), indicating that the PEG chains could impede the cellular uptake efficiencies of the compounds due to reduced lipophilicity. These observations are consistent with the flow cytometric data, which show that the cellular uptake of **BODIPY-Mito-5** and **BODIPY-Mito-6** was much lower than the other BODIPY compounds (Fig. 3B). By finely tuning the incubation concentration from 500 nM to 5 μM (**BODIPY-Mito-5**) and 25 μM (**BODIPY-Mito-6**), the cellular uptake efficiencies were substantially increased (Fig. 5A). Notably, **BODIPY-Mito-5** and **BODIPY-Mito-6** were also enriched in the mitochondria with good PCCs of 0.93 and 0.76, respectively (Fig. 5B). These results suggest that introduction of PEG chains could impede the cellular uptake. However, PEGylation does not pose a significant impact on the mitochondria-targeting properties of the compounds.

The control compound **BODIPY-Et** exhibited poor overlap with the MitoTracker (PCC = 0.56; Fig. 5C, top), demonstrating the significance of the phosphonium cation to direct the probes to the mitochondria. Co-localisation studies with Lipi-Blue, a commercial stain for lipid droplets, showed that **BODIPY-Et** was specifically enriched in the lipid droplets (PCC = 0.97; Fig. 5C, bottom) due to its neutral charge and high lipophilicity. Such a result is not surprising, and many lipophilic BODIPY derivatives have been found to efficiently target the lipid droplets.[40,41] Control compound **BODIPY-Et** could, therefore, warrant further studies for lipid droplet-related biological events.

After confirming the specific mitochondria-targeting properties of **BODIPY-Mito-*n***, we then examined the structural features that are important for a high MMP-dependent mitochondrial localisation. The cells were treated with the oxidative phosphorylation uncoupler carbonyl cyanide *m*-chlorophenylhydrazone (CCCP) after incubation with the **BODIPY-Mito-*n*** compounds to dissipate the transmembrane potential and depolarise the mitochondria. LSCM and flow cytometry were utilised to not only image the MMP sensitivity of the compounds, but also quantitatively measure the emission intensity changes. As revealed by LSCM, the CCCP treatment resulted in a substantial decrease in intracellular emission intensity for all six **BODIPY-Mito-*n*** compounds (Fig. 6A), demonstrating the strong dependence of the probes to MMP. This was further evidenced by flow cytometric analysis, which showed that the CCCP treatment led to 29–75% decrease in intracellular emission intensity (Fig. 6B and Table S2†). Since the fluorescence intensity of the probes was not quenched by CCCP (data not shown), the remarkable decrease in intracellular emission intensity suggests that the reduction in MMP led to the rapid release of the probes from the depolarised mitochondria. As a result, a substantial decrease in the mitochondrial accumulation of the probes was observed.

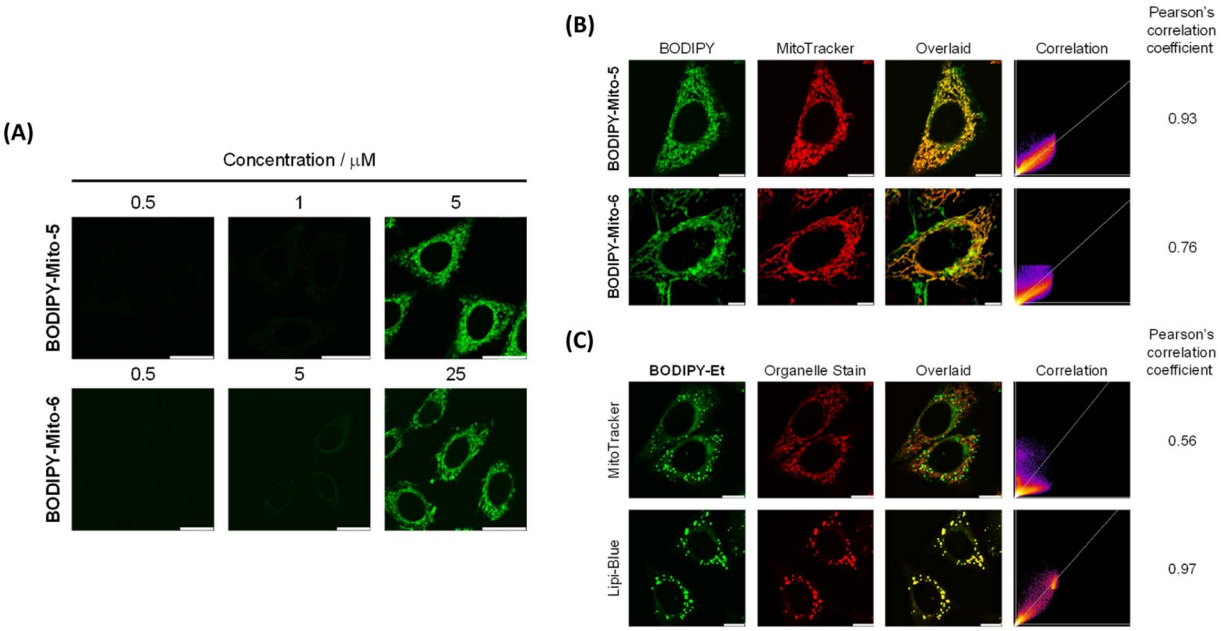

Fig. 5 (A) LSCM images of live HeLa cells incubated with **BODIPY-Mito-5** and **BODIPY-Mito-6** at different incubation concentrations for 1 h at 37 °C. $\lambda_{ex} = 488$ nm, $\lambda_{em} = 501–521$ nm. Scale bar = 25 μm. (B) LSCM images of live HeLa cells incubated with **BODIPY-Mito-5** (5 μM, 1 h; $\lambda_{ex} = 488$ nm, $\lambda_{em} = 501–521$ nm) and **BODIPY-Mito-6** (25 μM, 1 h; $\lambda_{ex} = 488$ nm, $\lambda_{em} = 501–521$ nm) and then MitoTracker Deep Red (100 nM, 30 min; $\lambda_{ex} = 635$ nm, $\lambda_{em} = 655–675$ nm) at 37 °C. Scale bar = 10 μm. (C) LSCM images of live HeLa cells incubated with **BODIPY-Et** (500 nM, 1 h; $\lambda_{ex} = 488$ nm, $\lambda_{em} = 501–521$ nm) and then MitoTracker Deep Red (100 nM, 30 min; $\lambda_{ex} = 635$ nm, $\lambda_{em} = 655–675$ nm) (top) or Lipi-Blue (500 nM, 30 min; $\lambda_{ex} = 405$ nm, $\lambda_{em} = 420–470$ nm) (bottom) at 37 °C. Scale bar = 10 μm.

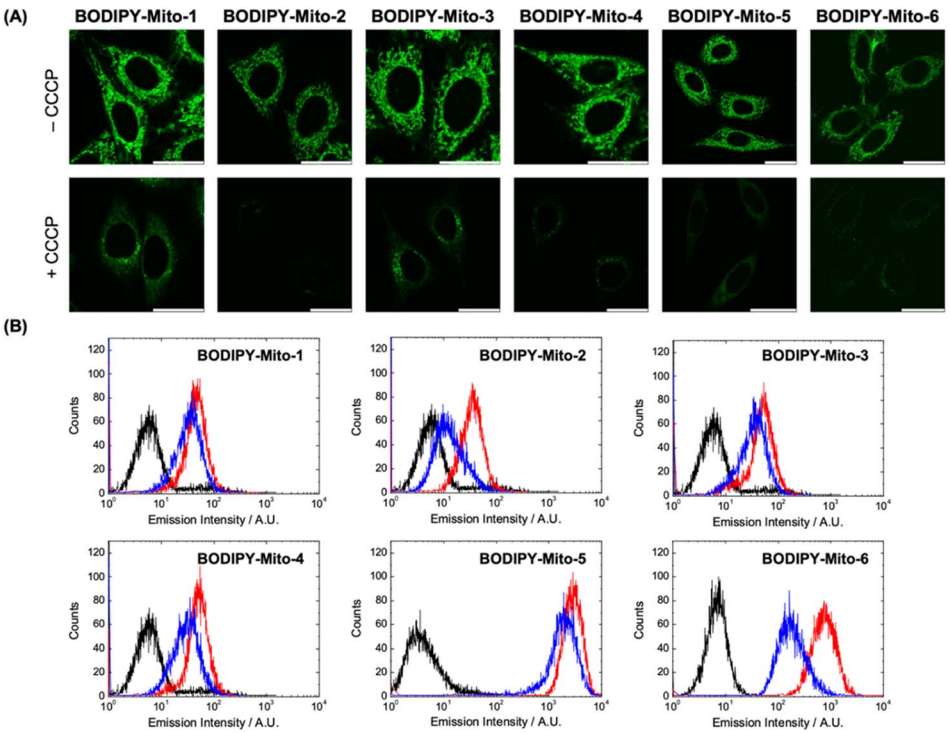

Fig. 6 (A) LSCM images of live HeLa cells incubated with **BODIPY-Mito-1–4** (500 nM, 1 h), **BODIPY-Mito-5** (5 μM, 1 h) or **BODIPY-Mito-6** (25 μM, 1 h) without (top) or with (bottom) post-treatment with CCCP (10 μM, 30 min) at 37 °C. $\lambda_{ex} = 488$ nm, $\lambda_{em} = 501–521$ nm. Scale bar = 25 μm. (B) Flow cytometric results of HeLa cells incubated with **BODIPY-Mito-*n***. The cells were treated with blank medium for 1 h (black); **BODIPY-Mito-1–4** (500 nM), **BODIPY-Mito-5** (5 μM) or **BODIPY-Mito-6** (25 μM) for 1 h (red); and **BODIPY-Mito-1–4** (500 nM), **BODIPY-Mito-5** (5 μM) or **BODIPY-Mito-6** (25 μM) for 1 h and then CCCP (10 μM) for 30 min (blue).

Among **BODIPY-Mito-1–4**, **BODIPY-Mito-2** showed the highest sensitivity to changes in MMP, which should be associated with the charge distribution on the phosphorus atom.[29] Furthermore, cells treated with the PEGylated **BODIPY-Mito-6** displayed a larger reduction in emission intensity (75%) when compared to its PEG-free (**BODIPY-Mito-4**; 40%) and DEG (**BODIPY-Mito-5**; 36%) counterparts. These results suggest that a longer PEG chain can minimize the non-specific interactions of the compound with mitochondrial proteins and membrane structures, enhancing the sensitivity of the compound towards changes in MMP.

Cytotoxicity of BODIPY-Mito-*n* analogues

Cytotoxicity is an important factor to consider when developing fluorescent probes for organelle-specific labelling and monitoring of dynamic processes in these subcellular organelles. As such, the cytotoxicity of **BODIPY-Mito-*n*** compounds was examined using the 3-(4,5-dimethylthiazol-2-yl)-2,5-diphenyltetrazolium bromide (MTT) assay. Considering that mitochondrial localisation of the probes could affect mitochondrial activity and lead to high cytotoxicity,[42] we chose to assess the cytotoxicity of the **BODIPY-Mito-*n*** compounds with a longer incubation period of 24 h.

The IC_{50} values of **BODIPY-Mito-1–4** were determined to be 5.0–6.7 μM (Table S3 and Fig. S7†), which are an order of magnitude higher than the imaging concentrations used (500 nM). Notably, the IC_{50} values of **BODIPY-Mito-5** (8.0 μM) and **BODIPY-Mito-6** (>50 μM) were higher than those of **BODIPY-Mito-1–4** (5.0–6.7 μM) due to the PEG pendants on the TPP^+ unit, showing that PEGylation can increase the biocompatibility of these compounds.

The control compound **BODIPY-Et** was also found to be essentially non-cytotoxic towards the cells (IC_{50} > 50 μM). These results highlight that the cellular localisation imposes an important factor in the cytotoxic activity of the BODIPY compounds, and the increased cytotoxicity of the **BODIPY-Mito-*n*** compounds is associated with their mitochondria-targeting capability. Nevertheless, the IC_{50} values of the **BODIPY-Mito-*n*** compounds (5.0–8.0 μM for **BODIPY-Mito-1–5** and >50 μM for **BODIPY-Mito-6**) are much higher than those that were used in the imaging experiments (*i.e.*, 500 nM for **BODIPY-Mito-1–4**, 5 μM for **BODIPY-Mito-5** and 25 μM for **BODIPY-Mito-6**; incubation time = 1 h) even with a prolonged incubation time (24 h). These results demonstrate that all the BODIPY compounds showed good biocompatibility and the **BODIPY-Mito-*n*** compounds are promising MMP-dependent mitochondria probes for fluorescence imaging applications.

Conclusions

Herein, we report the design, synthesis, photophysical properties and biological characterisation of a series of mitochondria-targeting BODIPY dyes. Six **BODIPY-Mito-*n*** compounds were synthesised in good yields that incorporated a range of cyclohexyl and/or phenyl substituents on the phosphonium cation as a strategy to optimise their mitochondrial localisation and MMP sensitivity.

All **BODIPY-Mito-*n*** derivatives showed pH-independent photophysical properties and displayed very high fluorescence quantum yields of between 0.59 and 0.72 in biologically relevant media.

Additionally, analogues bearing triarylphosphonium cations containing DEG (**BODIPY-Mito-5**) and PEG functionalities (**BODIPY-Mito-6**) showed improved water solubility, and extending the length of the chain was found to reduce the cytotoxicity of the probes (IC_{50} value increased from 8 μM to >50 μM).

Through the synthesis of the control compound **BODIPY-Et**, we demonstrated that lipophilic cations are critical to ensure effective mitochondria targeting, and the aromaticity of the lipophilic cations is not important for effective permeation through lipid membranes and accumulation in mitochondria.

Both cyclohexyl and phenyl moieties on the phosphonium cation can realise high MMP-dependent accumulation in the mitochondria, and all **BODIPY-Mito-*n*** analogues displayed excellent PCC values of between 0.76 and 0.96 in HeLa cells.

In BODIPY compounds incorporating cyclohexyl and/or phenyl substituents (**BODIPY-Mito-1–4**), **BODIPY-Mito-2** displayed the largest sensitivity to the MMP, where a 62% decrease in the emission intensity was seen in HeLa cells following CCCP-induced mitochondrial depolarisation. Such a result is in accordance with Archibald and co-workers, and was assigned to the cationic charge being localised on the phosphorus atom, rather than being delocalised on the aromatic ligands.[30]

However, across the **BODIPY-Mito-*n*** series, **BODIPY-Mito-6** not only displayed increased biocompatibility, but also enhanced sensitivity to the MMP, showing a 75% reduction in the emission intensity following mitochondrial depolarisation. Such a result highlights the potential of **BODIPY-Mito-6** to simultaneously label the mitochondria and monitor MMP changes in live cells.

Our results indicate that several factors play a crucial role in the design of mitochondria-specific probes with high MMP sensitivity. As such, **BODIPY-Mito-*n*** analogues have the potential to report on changes in mitochondrial function in cancer and cardiovascular disease. Additionally, we believe that our work will open new avenues for the design of mitochondria-targeting fluorescent probes in the future, providing improved alternatives to the widely used TPP^+ moiety for assessing mitochondrial activity and function.

Data availability

Data available in the ESI: instrumentation and methods, synthetic details, characterisation, analytical and photophysical data, and results of flow cytometry and cytotoxicity assays.†

Author contributions

E. R. H. W., L. C.-C. L., P. K.-K. L., K. K.-W. L. and N. J. L. designed the project. E. R. H. W. carried out the synthesis, characterisation, and UV-vis and fluorescence spectroscopy measurements of all the compounds. L. C.-C. L. and P. K.-K. L. carried out the biological characterisation and cellular studies. E. R. H. W., L. C.-C. L., P. K.-K. L., K. K.-W. L. and N. J. L.

analysed data. E. R. H. W., L. C.-C. L., P. K.-K. L., K. K.-W. L. and N. J. L. wrote the manuscript.

Conflicts of interest

There are no conflicts of interest to declare.

Acknowledgements

We acknowledge the funding support from "Laboratory for Synthetic Chemistry and Chemical Biology" under the Health@InnoHK Program launched by Innovation and Technology Commission, The Government of Hong Kong Special Administrative Region of the People's Republic of China.

References

1 L. D. Zorova, V. A. Popkov, E. Y. Plotnikov, D. N. Silachev, I. B. Pevzner, S. S. Jankauskas, V. A. Babenko, S. D. Zorov, A. V. Balakireva, M. Juhaszova, S. J. Sollott and D. B. Zorov, *Anal. Biochem.*, 2018, **552**, 50–59.
2 J. B. Spinelli and M. C. Haigis, *Nat. Cell Biol.*, 2018, **20**, 745–754.
3 C. Cadonic, M. G. Sabbir and B. C. Albensi, *Mol. Neurobiol.*, 2016, **53**, 6078–6090.
4 N. Sun, R. J. Youle and T. Finkel, *Mol. Cell*, 2016, **61**, 654–666.
5 J. Zielonka, J. Joseph, A. Sikora, M. Hardy, O. Ouari, J. Vasquez-Vivar, G. Cheng, M. Lopez and B. Kalyanaraman, *Chem. Rev.*, 2017, **117**, 10043–10120.
6 M. P. Murphy and R. A. J. Smith, *Annu. Rev. Pharmacol. Toxicol.*, 2007, **47**, 629–656.
7 M. P. Murphy, *Biochim. Biophys. Acta, Bioenerg.*, 2008, **1777**, 1028–1031.
8 J. S. Modica-Napolitano and J. R. Aprille, *Adv. Drug Deliv. Rev.*, 2001, **49**, 63–70.
9 X. Zhang, S. Sarkar, A. Ashokan, B. Surnar, N. Kolishetti and S. Dhar, *Bioconjugate Chem.*, 2023, **34**, 1122–1129.
10 J. Maddahi, H. Kiat, K. F. Van Train, F. Prigent, J. Friedman, E. V. Garcia, N. Alazraki, E. G. DePuey, K. Nichols and D. S. Berman, *Am. J. Cardiol.*, 1990, **66**, E55–E62.
11 A. Haslop, A. Gee, C. Plisson and N. Long, *J. Label. Compd. Radiopharm.*, 2013, **56**, 313–316.
12 S. P. McCluskey, A. Haslop, C. Coello, R. N. Gunn, E. W. Tate, R. Southworth, C. Plisson, N. J. Long and L. A. Wells, *J. Nucl. Med.*, 2019, **60**, 1750–1756.
13 A. J. Smith, B. E. Osborne, G. P. Keeling, P. J. Blower, R. Southworth and N. J. Long, *Dalton Trans.*, 2020, **49**, 1097–1106.
14 B. E. Osborne, T. T. C. Yue, E. C. T. Waters, F. Baark, R. Southworth and N. J. Long, *Dalton Trans.*, 2021, **50**, 14695–14705.
15 E. R. H. Walter, S. M. Cooper, J. J. Boyle and N. J. Long, *Dalton Trans.*, 2021, **50**, 14486–14497.
16 F. Sivandzade, A. Bhalerao and L. Cucullo, *Bio-Protoc.*, 2019, **9**, e3128.
17 A. Baracca, G. Sgarbi, G. Solaini and G. Lenaz, *Biochim. Biophys. Acta, Bioenerg.*, 2003, **1606**, 137–146.
18 J. Lin, K. Yang and E. J. New, *Org. Biomol. Chem.*, 2021, **19**, 9339–9357.
19 J. Gemen, J. Ahrens, L. J. W. Shimon and R. Klajn, *J. Am. Chem. Soc.*, 2020, **142**, 17721–17729.
20 E. Bassan, A. Gualandi, P. G. Cozzi and P. Ceroni, *Chem. Sci.*, 2021, **12**, 6607–6628.
21 J.-L. Wang, L. Zhang, M.-J. Zhao, T. Zhang, Y. Liu and F.-L. Jiang, *ACS Appl. Bio Mater.*, 2021, **4**, 1760–1770.
22 H.-Y. Kwon, J.-Y. Kim, J. Y. Lee, J. K. H. Yam, L. D. Hultqvist, W. Xu, M. Rybtke, T. Tolker-Nielsen, J.-J. Kim, N.-Y. Kang, L. Yang, S.-J. Park, M. Givskov and Y.-T. Chang, *Chem. Commun.*, 2018, **54**, 11865–11868.
23 D. Kand, L. Pizarro, I. Angel, A. Avni, D. Friedmann-Morvinski and R. Weinstain, *Angew. Chem., Int. Ed.*, 2019, **58**, 4659–4663.
24 S. Zhang, T. Wu, J. Fan, Z. Li, N. Jiang, J. Wang, B. Dou, S. Sun, F. Song and X. Peng, *Org. Biomol. Chem.*, 2013, **11**, 555–558.
25 B. Sui, S. Tang, A. W. Woodward, B. Kim and K. D. Belfield, *Eur. J. Org. Chem.*, 2016, **2016**, 2851–2857.
26 H. Yuan, H. Cho, H. H. Chen, M. Panagia, D. E. Sosnovik and L. Josephson, *Chem. Commun.*, 2013, **49**, 10361–10363.
27 K. Chansaenpak, H. Wang, M. Wang, B. Giglio, X. Ma, H. Yuan, S. Hu, Z. Wu and Z. Li, *Chem.–Eur. J.*, 2016, **22**, 12122–12129.
28 G. Cheng, J. Fan, W. Sun, K. Sui, X. Jin, J. Wang and X. Peng, *Analyst*, 2013, **138**, 6091–6096.
29 J. Miao, Y. Huo, Q. Liu, Z. Li, H. Shi, Y. Shi and W. Guo, *Biomaterials*, 2016, **107**, 33–43.
30 S. Nigam, B. P. Burke, L. H. Davies, J. Domarkas, J. F. Wallis, P. G. Waddell, J. S. Waby, D. M. Benoit, A.-M. Seymour, C. Cawthorne, L. J. Higham and S. J. Archibald, *Chem. Commun.*, 2016, **52**, 7114–7117.
31 L. H. Davies, R. W. Harrington, W. Clegg and L. J. Higham, *Dalton Trans.*, 2014, **43**, 13485–13499.
32 L. H. Davies, B. Stewart, R. W. Harrington, W. Clegg and L. J. Higham, *Angew. Chem., Int. Ed.*, 2012, **51**, 4921–4924.
33 T. Rousseau, A. Cravino, T. Bura, G. Ulrich, R. Ziessel and J. Roncali, *Chem. Commun.*, 2009, 1673–1675.
34 P. Didier, G. Ulrich, Y. Mély and R. Ziessel, *Org. Biomol. Chem.*, 2009, **7**, 3639–3642.
35 B. Yuan, H. Wu, H. Wang, B. Tang, J.-F. Xu and X. Zhang, *Angew. Chem., Int. Ed.*, 2021, **60**, 706–710.
36 T. James and N. P. Barwell, WO2012095628A1, 2012.
37 M. Jiang, J. Wu, W. Liu, H. Ren, W. Zhang, C.-S. Lee and P. Wang, *Chem.–Eur. J.*, 2021, **27**, 11195–11204.
38 J. H. Brannon and D. Magde, *J. Phys. Chem.*, 1978, **82**, 705–709.
39 T. I. Rokitskaya, E. A. Kotova, V. B. Luzhkov, R. S. Kirsanov, E. V. Aleksandrova, G. A. Korshunova, V. N. Tashlitsky and Y. N. Antonenko, *Biochim. Biophys. Acta, Biomembr.*, 2021, **1863**, 183483.
40 Y. Zhao, W. Shi, X. Li and H. Ma, *Chem. Commun.*, 2022, **58**, 1495–1509.
41 J. Zhu, N. K. Tan, K. Kikuchi, A. Kaur and E. J. New, *Analysis Sensing*, 2024, **4**, e202300049.
42 T. Zhao, X. Liu, S. Singh, X. Liu, Y. Zhang, J. Sawada, M. Komatsu and K. D. Belfield, *Bioconjugate Chem.*, 2019, **30**, 2312–2316.